JOURNAL OF BACTERIOLOGY, Mar. 1994, p. 1711–1717
0021-9193/94/$04.00+0

Vol. 176, No. 6

The Essential Virulence Protein VirB8 Localizes to the Inner Membrane of *Agrobacterium tumefaciens*

YVONNE R. THORSTENSON[1]† AND PATRICIA C. ZAMBRYSKI*

Plant Biology Department, University of California, Berkeley, California 94720

Received 7 September 1993/Accepted 12 January 1994

Agrobacterium tumefaciens **genetically transforms plant cells by transferring a specific DNA fragment from the bacterium through several biological membranes to the plant nucleus where the DNA is integrated. This complex DNA transport process likely involves membrane-localized proteins in both the plant and the bacterium. The 11 hydrophobic or membrane-localized proteins of the *virB* operon are excellent candidates to have a role in DNA export from agrobacteria. Here, we show by Tn*phoA* mutagenesis and immunogold electron microscopy that one of the VirB proteins, VirB8, is located at the inner membrane. The observation that a *virB8*::Tn*phoA* fusion restores export of alkaline phosphatase to the periplasm suggests that VirB8 spans the inner membrane. Immunogold labeling of VirB8 was detected on the inner membrane of *vir*-induced *A. tumefaciens* by transmission electron microscopy. Compared with that of the controls, VirB8 labeling was significantly greater on the inner membrane than on the other cell compartments. These results confirm the inner membrane localization of VirB8 and strengthen the hypothesis that VirB proteins help form a transfer DNA export channel or gate.**

The DNA transfer from the soil bacterium *Agrobacterium tumefaciens* to plants that results in crown gall tumor formation is the only known naturally occurring example of interkingdom DNA transfer. The components necessary for DNA transfer and plant transformation are encoded on two regions of the extrachromosomal tumor-inducing (Ti) plasmid (for reviews, see references 53 and 55). The first region, the transfer DNA (T-DNA), is bordered by direct repeats and contains genes encoding plant hormone-producing enzymes which cause neoplastic growth of transformed plant cells. The second region, the virulence (*vir*) region, encodes gene products involved in generating, processing, packaging, transporting, and nuclear targeting of the T-DNA. The two-component regulatory system of VirA and VirG responds to plant signal molecules to activate transcription of *vir* genes. These *vir* gene products, in turn, produce and transport the T-DNA to the plant cell. Two proteins of *virD*, VirD1 and VirD2, nick at the T-DNA borders and unwind the single-stranded T-DNA (T-strand). The T-strand then is packaged for transport as a DNA-protein complex (T-complex). VirD2 covalently binds to the 5′ end, while VirE2 cooperatively coats the single-stranded DNA.

A critical step of plant transformation by *A. tumefaciens*, namely the mechanism of T-complex export from the bacterium, is yet to be elucidated. Since the T-complex is large and long, it likely is transported through a specialized pore or channel. To date, the best candidates to form a T-complex-specific transport channel are the products of the *virB* locus. Nine of the eleven proteins encoded by the *virB* operon are predicted to be membrane localized (21, 37, 43, 46, 47). All of the VirB proteins that have been tested individually (VirB4, VirB8, VirB9, VirB10, and VirB11) are essential for virulence (2, 12, 36, 39, 48). At least nine VirB proteins have been localized to the bacterial membranes by cell fractionation: VirB3 (43a), VirB4 (2, 15, 36), VirB10 (49), VirB11 (7), VirB2, -3, and -9 (34), and VirB1, -4, -5, -8, -9, -10, and -11 (44). Another essential virulence protein, VirD4, was also localized to the bacterial inner membrane (29) and might interact with VirB proteins to form the exit pore or channel required for T-complex transport.

Examination of VirB proteins in subcellular fractions of *A. tumefaciens* was useful to identify them as membrane-localized proteins. Taking advantage of our collection of antibodies against VirB proteins, we next examined the in situ localization of VirB proteins by immunogold electron microscopy. We undertook this technically demanding approach expecting to observe the distribution of several VirB proteins within the bacterial membranes, for example, at points of contact between the inner and outer membranes and clustering at specific sites corresponding to one or a few T-complex transport channels. These expectations were not fulfilled. We tested eight polyclonal antibodies recognizing seven different VirB proteins, and only one of them, the VirB8 antibody, gave a sufficiently strong and reproducible signal for our analyses.

VirB8 is a 26-kDa protein encoded by the eighth open reading frame of the *virB* operon. Amino acid sequence analysis predicts that one hydrophobic stretch of about 20 amino acids in the amino-terminal third of the protein may form a transmembrane alpha helix that spans the membrane (see Fig. 1 and reference 20). Along with other VirB proteins, VirB8 has homology to proteins believed to be involved in conjugal transfer of IncW plasmids (18) and in export of pertussis toxin in *Bordetella pertussis* (11, 35). Several VirB proteins (VirB2, VirB3, VirB4, VirB5, VirB10, and VirB11) also have homology with transfer proteins of IncP plasmids (23). The similarity of VirB proteins to proteins involved in the transport of conjugative plasmids was not surprising, because transfer of both conjugative plasmids and T-DNA involves single-stranded DNA intermediates (41). In addition, the nick region of IncP RP4 and T-DNA borders share a 12-bp consensus sequence (10, 50, 51) and the *A. tumefaciens* VirD2 and IncP TraI proteins involved in DNA nicking and binding to the 5′ end of the single-stranded DNA transfer molecules are homologous (30, 31, 57).

VirB8 is required for the virulence of *A. tumefaciens* on *Kalanchoe* species (12) but its function is not known. In

* Corresponding author.
† Present address: Carnegie Institution, Department of Plant Biology, Stanford, CA 94305.

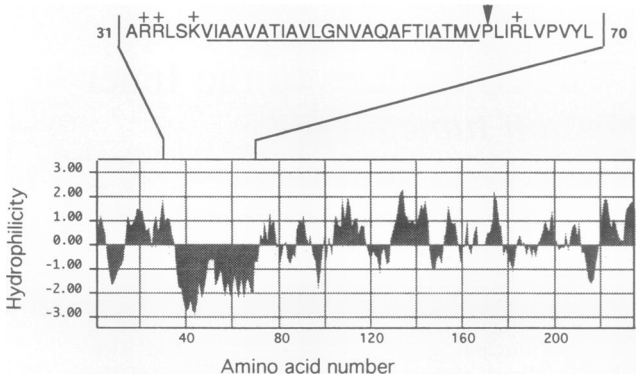

FIG. 1. Position of Tn*phoA* insertion in the VirB8 amino acid sequence shown with respect to the hydropathy profile. The amino acid position of VirB8 (21) is indicated on the horizontal axis. The single-letter amino acid sequence is shown for amino acids 31 to 70. Positively charged amino acids (+) are indicated. A stretch of hydrophobic amino acids (underlined sequence) represents the predicted membrane-spanning region. The site of Tn*phoA* fusion with *virB8* (arrowhead) is also indicated. The hydropathy profile was performed by the method of Kyte and Doolittle (22), with a window size of 7 amino acids. Hydrophobic regions are indicated by more negative hydrophilicity values (vertical axis).

subcellular fractions of *A. tumefaciens*, VirB8 was mainly found associated with the inner membrane fractions but was also associated with the outer membrane fractions (44). The less-than-total specificity of the localization was attributed to cross-contamination of the fractions that is inherent in the fractionation procedure. Here, we provide direct evidence, using immunogold electron microscopy and Tn*phoA* mutagenesis of VirB8, that VirB8 localizes exclusively to the inner membrane.

MATERIALS AND METHODS

Tn*phoA* mutagenesis of VirB8. Tn*phoA* mutagenesis was accomplished with the vector λTnPhoA (16) which was propagated in *Escherichia coli* LE392 (33). The target plasmid for Tn*phoA* mutagenesis was pVirB8 (44) containing *virB8* in pGEMEX-2, a protein overexpression vector (Promega). Mutagenesis was carried out for 1 h at 30°C by adding λTnPhoA at a multiplicity of infection of 0.5 to *E. coli* MM294A (25) at an optical density at 600 nm of 0.5 to 1.0. Following mutagenesis, *E. coli* colonies containing mutagenized plasmids were directly plated for selection on Luria-Bertani (LB) plates containing 30 μg of kanamycin. A single pool of DNA from the kanamycin-resistant colonies was isolated by alkaline lysis and polyethylene glycol purification (25). The mutagenized DNA was then transformed into the alkaline phosphatase-negative *E. coli* strain CC118 containing the helper plasmid pGP-1 (42). Alkaline phosphatase-positive colonies were detected as blue colonies on LB plates containing 40 μg of the chromogenic phosphatase substrate 5-bromo-4-chloro-3-indolylphosphate (X-P) per liter, as described previously (4), and alkaline phosphatase activity was quantified by the method of Stachel et al. (38), except that X-P was used instead of X-Gal (5-bromo-4-chloro-3-indolyl-β-D-galactopyranoside). Double-stranded templates of plasmid DNA from each blue colony were isolated by an alkaline lysis method (25), annealed to the Tn*phoA* complementary primer 3′CTAGTCTGACGG CGAG5′ by the method of Chen and Seeburg (5), and sequenced by a dideoxy chain termination method using Sequenase (United States Biochemicals).

Immunogold electron microscopy. *A. tumefaciens* A3850 (56) and Mx306 (39) were grown, and *vir* gene expression was induced with 100 μM acetosyringone (Aldrich) as described elsewhere (8, 40). Fixation by freeze substitution of induced and uninduced *A. tumefaciens* cells was performed essentially as described previously (58) except that 0.5 to 1.0% instead of 3% glutaraldehyde was used. The tissue was embedded in the acrylic resin LR White (Ted Pella). Formvar-coated 200-mesh nickel grids (Ted Pella) were carbon coated and treated by ion discharge in a Denton 502A vacuum evaporator. Ultrathin (silver) sections of plastic-embedded cells were cut with an MT-7 or MT6000 ultramicrotome (LKB) and picked up on Formvar grids.

Grids containing bacterial sections were labeled by floating them sequentially, section side down, on 25- to 30-μl drops of each solution as follows: (i) 0.1% glycine or 2% sodium borohydride for 15 min to quench unreacted aldehyde groups (optional), (ii) blocking agent (described below) for 15 to 30 min, (iii) primary antibody (described below) diluted 1:500 in blocking agent at 4°C overnight, (iv) 0.5 M NaCl in phosphate-buffered saline, three times for 5 min each, (v) secondary antibody buffer (1.0% bovine serum albumin in 10 mM Tris [pH 7.5]–150 mM NaCl [TBS]) for 5 min, (vi) secondary antibody (10-nm-diameter gold-conjugated goat anti-rabbit immunoglobulin G [Ted Pella]) diluted 1:50 in secondary antibody buffer for 40 to 60 min, (vii) TBS, three times for 5 min each, (viii) 1% glutaraldehyde in TBS for 15 min, (ix) distilled water at least twice for 5 to 10 min each, and (x) 2% aqueous uranyl acetate for 15 to 20 min. The grids were then washed by submersion in a beaker of distilled water and air dried. The primary antibody was either polyclonal antiserum against VirB1, VirB4, VirB5, VirB8, VirB9, VirB10, or VirB11 protein (44), VirE2 protein (9), or preimmune serum. All steps were performed at room temperature except where indicated. Labeled cells were observed in the JEOL 100CX or Zeiss 109 transmission electron microscope operating at 80 kV and photographed. The blocking agent for immunogold labeling was 5% normal goat serum or 2% ovalbumin supplemented with 0.2% Tween 20.

The number of gold particles were counted in all longitudinal sections (length greater than twice the width) that were observed. The maximum expected distance between a gold particle on the secondary antibody and a labeled antigen is 30 nm, corresponding to the length of the primary-secondary antibody complex (19). Using a conservative estimate, we counted gold particles that were within 10 nm (one gold particle width) on either side of the membrane as being localized to the inner membrane. Since the width of the inner membrane itself was 10 nm, the total width of the band counted as inner membrane was 30 nm. All other gold particles within a cell section were counted as non-inner membrane localized.

To calculate the average cell area, images of longitudinally sectioned cells were imported from photographic negatives by a video camera (Javelin Ultrichip HiRes CCD) connected to a Macintosh IIfx computer with Image 1.47 (National Institutes of Health). By tracing the perimeter of the inner and outer membranes in Canvas 3.0 (Deneba Systems, Inc.) using the Bezier curve option, two polygons were created and measured. One had an area equal to the total area of the cell section, and the other one had an area equal to the area of the sectioned cytoplasm. The area of the inner membrane was calculated as the perimeter of the inner membrane multiplied by 30 nm (see the explanation above). The area corresponding to the non-

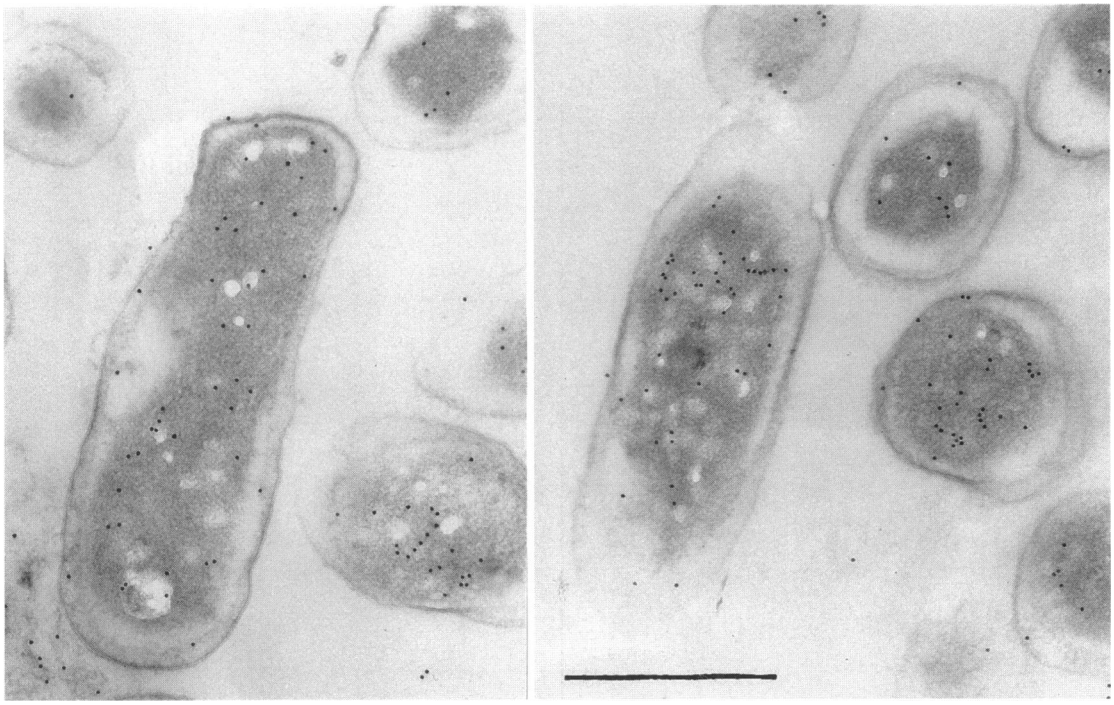

FIG. 2. Electron micrographs of an independent control, showing localization of VirE2 in ultrathin sections of *A. tumefaciens*. Two representative views of VirE2-labeled sections of *vir*-induced strain A3850. *vir* gene expression was induced by the addition of acetosyringone to the growth medium. VirE2 was visualized first with VirE2-specific antiserum as a primary antibody followed by secondary antibody conjugated to 10-nm-diameter gold particles (black dots). Bar = 1 μm.

inner membrane compartments was calculated as the total area of the section minus the area of the inner membrane.

Statistical analyses were performed with Systat 5.2.1 (Systat Inc.). The data were used to test the statistical null hypothesis that the gold particle concentration associated with the inner membrane corresponds to the concentration of the other cell compartments. A generalized likelihood ratio test based on the frequency distributions in the different cell compartments allowed a chi-square test of this hypothesis. The chi-square values have degrees of freedom equal to the number of sectioned cells counted. The chances of observing a chi-square value larger than those reported are given as *P* values.

RESULTS AND DISCUSSION

***virB*::Tn*phoA* fusions.** To test the hypothesis that VirB8 localizes to the membrane, we randomly mutagenized *virB8* with the transposon Tn*phoA*. Tn*phoA* is a Tn*5* derivative that contains a truncated form of the alkaline phosphatase gene *phoA* in the left inverted repeat of the transposon (26). The phosphatase gene lacks both a promoter and the signal sequences necessary for transport of the enzyme to the periplasm where it is functional (17). Insertion of Tn*phoA* in the correct reading frame and orientation, i.e., after a transmembrane or membrane signal sequence in the target protein, is expected to yield *E. coli* colonies with phosphatase activity (26). The generation of translational fusions with Tn*phoA* has been used as a technique to identify membrane or periplasmic proteins and to determine the topology of membrane proteins such as VirA (28, 54) or VirB10 (49).

We produced Tn*phoA* insertions in a plasmid containing *virB8* and tested them for phosphatase activity in a phosphatase deletion strain of *E. coli*. We obtained 12 isolates containing insertions of Tn*phoA* in the target plasmid that restored phosphatase activity. Alkaline phosphatase activity was measured for 7 of the 12 isolates. The average activity was 63 ± 12 U/min, compared with 3.5 U/min for an alkaline phosphatase-negative control. Nucleotide sequence analysis revealed that all Tn*phoA* insertions were in the correct reading frame with respect to *virB* and were at the same position in *virB* DNA, resulting in a fusion protein that contains the first 60 amino acids of VirB8, a novel amino acid at position 61, and the alkaline phosphatase protein of Tn*phoA* (Fig. 1). The insertion site is at the end of the predicted membrane-spanning region of hydrophobic amino acids in VirB8 (Fig. 1). The cluster of three positively charged amino acids upstream of the hydrophobic stretch may function to orient the amino terminus of VirB8 in the cytoplasm (for a review, see reference 3). The isolation of a *virB8*::Tn*phoA* fusion that restores alkaline phosphatase activity confirms earlier evidence that VirB8 is localized to the bacterial membrane and suggests that its orientation in the inner membrane may be similar to that of VirB10 (49).

The finding that the 12 isolates of Tn*phoA* insertions were in the same position in VirB8 was surprising, since the transposon from which Tn*phoA* was derived, Tn*5*, has been reported to have a low specificity for insertion in DNA (14). In contrast, in parallel experiments where we mutagenized plasmids containing other *virB* genes (*virB2*, *virB3*, and *virB5*), we obtained a more random distribution of insertion sites (12 insertions in five different sites [data not shown]). Thus, there may be a "hot spot" for insertion events at this particular site in *virB8*. Another group reported a similar result from using Tn*phoA* mutagenesis of gene IV of the filamentous bacteriophage f1, where 85% of the insertions were at the same site (32).

FIG. 3

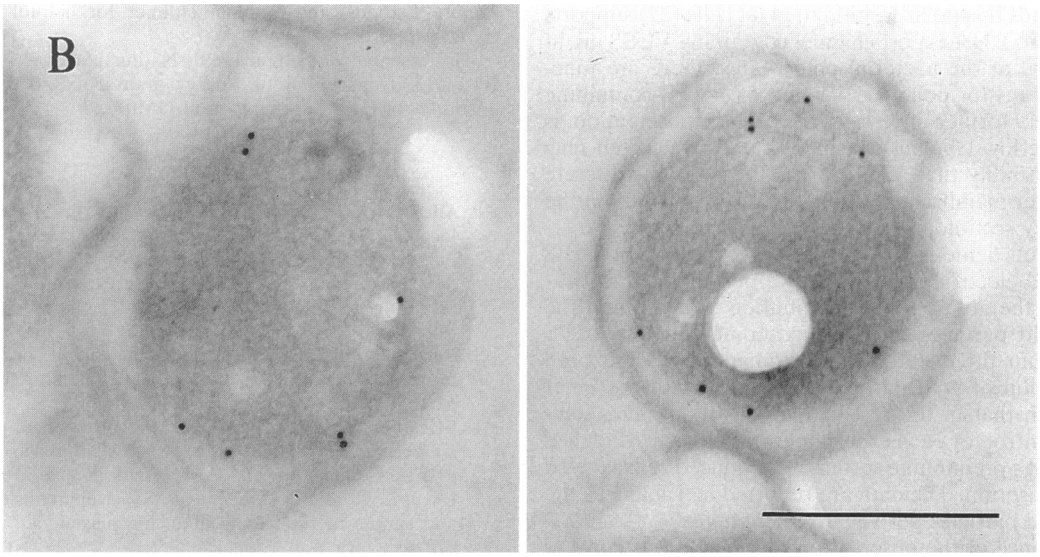

FIG. 3. Electron micrographs of ultrathin sections of *A. tumefaciens* labeled with VirB8 antiserum. Induction of A3850 for *vir* gene expression and immunogold labeling with VirB8 antiserum was done as described for Fig. 2. Control experiments which included *vir*-induced A3850 labeled with preimmune serum and uninduced A3850 labeled with VirB8 showed less than one gold particle per section on the inner membrane. Bars = 300 nm. (A) Longitudinal sections. The top two panels are representative of cells from experiment I in Table 1. The bottom two panels are representative of experiments II and III in Table 1. (B) Representative cross sections of cells from experiment II.

Immunogold labeling of VirB8. The ability to directly observe the in situ localization of proteins by immunogold labeling is an obvious advantage over the localization of proteins by cell fractionation. Immunogold labeling potentially reveals the location of antigens in relation to the overall cell architecture and their distribution (i.e., uniform, random, or clustered) within a cell compartment. For example, immunogold electron microscopy was used to demonstrate the polar distribution of a membrane-localized chemoreceptor complex in *Caulobacter crescentus* (1, 24).

TABLE 1. Gold concentration at inner membrane or non-inner membrane in immunolabeled ultrathin sections of *A. tumefaciens*[a]

Expt and treatment	No. of sections observed	Gold concn (particles/μm^2)	
		Inner membrane	Non-inner membrane
Expt I			
VirB8 label	68	13.5	1.9
Preimmune control	45	0.8	0.5
Expt II			
VirB8 label	123	12.5	4.4
Preimmune control	111	3.0	3.3
Expt III			
VirB8 label	83	18.9	5.7
Uninduced control	147	3.5	3.4

[a] Gold label was counted in all longitudinal sections observed. Gold particles per square micrometer were calculated by dividing the total number of gold particles observed on the inner membrane (IM) or non-inner membrane (NIM) by the total area of IM or NIM observed (number of sections observed × average area of IM or NIM). Average areas of sections through the IM or NIM were determined independently for samples from two different fixations because the cell shape was slightly different in each. In the sections from the first fixation (experiment I and the top two panels of Fig. 3A), the area of IM, averaged from 17 sections, was 0.11 μm^2 per cell and NIM area was 0.62 μm^2 per cell. In the sections from the second fixation (experiments II and III and the bottom two panels of Fig. 3A), the areas were 0.09 and 0.35 μm^2 per cell, respectively, averaged from 22 sections.

We analyzed the abilities of polyclonal antisera against seven different VirB proteins to reveal a pattern of antigen distribution on ultrathin sections of *vir*-induced *A. tumefaciens*. Antibodies bound to VirB proteins were detected by gold-conjugated secondary antibody and transmission electron microscopy. Signals produced by all but one of the antibodies were difficult to detect, either because they were too weak or the background was too strong. Only antiserum raised against VirB8 protein produced a sufficiently strong and clean signal to warrant further analysis.

Immunogold labeling of the *A. tumefaciens* virulence protein VirE2 was used as an independent control for subcellular localization of proteins in *vir*-induced cells. VirE2 is known to be abundant in the cytoplasm, as determined by cell fractionation (6) and as predicted by its function in binding single-stranded T-strand DNA (6, 8, 13). As expected, the gold particles labeling VirE2 protein were mainly found in the cytoplasm (Fig. 2). Interestingly, we noticed strings of label that might correspond to VirE2-coated single-stranded nucleic acid in two different VirE2-expressing cell types. Because the strings were observed both in a VirD2 mutant strain lacking T-strands (Mx306 [data not shown]) and in a wild-type strain containing T-strands (A3850), this pattern of labeling may represent labeling of T-complexes in wild-type cells and nonspecific labeling of single-stranded nucleic acids, such as the abundant mRNA population, in cells lacking T-strands.

Immunogold labeling of VirB8 was distinct from that of VirE2. The overall density of labeling was reduced, and the label was concentrated on the inner membrane (Fig. 3). Intriguingly, the label associated with the inner membrane tended to be most dense at the poles of the cells. The statistical significance of this result is difficult to assess, since the labeling frequency is low and there is a very small sample size, i.e., it is relatively improbable that a random section will have occurred exactly through both poles of the cell. The observation that *A.*

tumefaciens binds in a polar fashion to plant cells (27) supports the idea that a T-DNA export channel containing VirB8 might be concentrated at the bacterial poles. Since there are functional implications for polar localization of a VirB-containing export channel, further investigation of this observation is warranted. The low labeling density was unexpected but may reflect the possibility that VirB8 is localized only at discrete sites of the inner membrane that might not be exposed on the surface of every section and therefore is not detected.

To conclusively demonstrate the in situ localization of VirB8 by immunogold electron microscopy, we performed a statistical analysis of the gold particle distribution. We counted the number of gold particles in 577 longitudinal sections of *A. tumefaciens* from three different experiments and compared the concentration of gold particles associated with the inner membrane with that in the rest of the cell (non-inner membrane). The control for each experiment was either *vir*-induced cells labeled with preimmune serum or uninduced cells labeled with VirB8 antiserum. The data are reported in Table 1 as the number of gold particles per square micrometer.

The significance of the observation that VirB8 was concentrated on the inner membrane of *A. tumefaciens* was demonstrated with a chi-square test of data combined from the three experiments. To combine the data, we first demonstrated that there were no statistically significant differences between the three different experiments in the distribution of the label (data not shown). We then compared the concentration of gold particles associated with the inner membrane in VirB8-labeled sections with that of the controls, repeating the comparison for the non-inner membrane compartments. The difference in the concentration of gold particles in the non-inner membrane compartments in VirB8-labeled cells and the concentration in the negative controls was statistically insignificant (3.81 versus 2.67 gold particles per μm^2; $P > 0.05$). In contrast, the quantity of the label on the inner membrane of VirB8-labeled sections of *A. tumefaciens*, 12.8 gold particles per μm^2, was significantly greater ($P < 0.001$) than that of the controls, with 2.85 gold particles per μm^2. These statistical analyses support the notion that VirB8 is localized on the inner membrane of *vir*-induced cells.

The inner membrane localization of VirB8, along with its requirement for virulence (12) and its homology to proteins of other transport machinery (18, 52), strongly suggests that VirB8 is a component of the T-DNA export machinery. The homologies of VirB proteins with the conjugative transfer proteins do not yet reveal how VirB proteins function to transport T-DNA, because so little is known about conjugative transfer mechanisms themselves. However, the intriguing homologies of VirB proteins with pertussis toxin export machinery suggest VirB-encoded channels may principally function to transport protein. Indeed, in the process of T-strand production, the DNA becomes covalently attached to the VirD2 protein and coated with VirE2 single-stranded binding protein. In essence, the DNA is hidden and only protein is exposed for transport. Just as a DNA-protein conjugate could be imported into mitochondria via the protein import pathway (45), the T-complex might exit the bacterium through a protein export channel.

ACKNOWLEDGMENTS

We sincerely appreciate assistance from Gail McLean for critically reading the manuscript and suggesting many improvements. We also thank Todd Zorick, Caroline Schooley, and Doug Davis for technical advice with electron microscopy techniques; Ives Dessaux for providing λTnPhoA; Vitaly Citovsky for providing VirE2 antiserum; Cal Kado for sending preprints; and Gretchen Kuldau, Janine Maddock, Denise Lapidus, and Stephan Hillmer for helpful discussions and moral support.

This research was supported by National Science Foundation grant 89-15613, Department of Energy grant 88ER13882, and National Institutes of Health training grant GM07127.

REFERENCES

1. **Alley, M. R. K., J. R. Maddock, and L. Shapiro.** 1992. Polar localization of a bacterial chemoreceptor. Genes Dev. **6**:825–836.
2. **Berger, B. R., and P. J. Christie.** 1993. The *Agrobacterium tumefaciens virB4* gene product is an essential virulence protein requiring an intact nucleoside triphosphate-binding domain. J. Bacteriol. **175**:1723–1734.
3. **Boyd, D., and J. Beckwith.** 1990. The role of charged amino acids in the localization of secreted and membrane proteins. Cell **62**:1031–1033.
4. **Brickman, E., and J. Beckwith.** 1975. Analysis of the regulation of *Escherichia coli* alkaline phosphatase synthesis using deletions and ϕ80 transducing phages. J. Mol. Biol. **96**:307–316.
5. **Chen, E. Y., and P. H. Seeburg.** 1985. Supercoil sequencing: a fast and simple method for sequencing plasmid DNA. DNA **4**:165–170.
6. **Christie, P. J., J. E. Ward, S. C. Winans, and E. W. Nester.** 1988. The *Agrobacterium tumefaciens virE2* gene product is a single-stranded-DNA-binding protein that associates with T-DNA. J. Bacteriol. **170**:2659–2667.
7. **Christie, P. J., J. J. Ward, M. P. Gordon, and E. W. Nester.** 1989. A gene required for transfer of T-DNA to plants encodes an ATPase with autophosphorylating activity. Proc. Natl. Acad. Sci. USA **86**:9677–9681.
8. **Citovsky, V., G. De Vos, and P. Zambryski.** 1988. Single-stranded DNA binding protein encoded by the *virE* locus of *Agrobacterium tumefaciens*. Science **240**:501–504.
9. **Citovsky, V., J. Zupan, D. Warnick, and P. Zambryski.** 1992. Nuclear localization of *Agrobacterium* VirE2 protein in plant cells. Science **256**:1802–1805.
10. **Cook, D. M., and S. K. Farrand.** 1992. The *oriT* region of the *Agrobacterium tumefaciens* Ti plasmid pTiC58 shares DNA sequence identity with the transfer origins of RSF1010 and RK2/RP4 and with T-region borders. J. Bacteriol. **174**:6238–6246.
11. **Covacci, A., and R. Rappuoli.** 1993. Pertussis toxin export requires accessory genes located downstream from the pertussis toxin operon. Mol. Microbiol. **8**:429–434.
12. **Dale, E. M., A. N. Binns, and J. J. Ward.** 1993. Construction and characterization of Tn*5virB*, a transposon that generates nonpolar mutations, and its use to define *virB8* as an essential virulence gene in *Agrobacterium tumefaciens*. J. Bacteriol. **175**:887–891.
13. **Das, A.** 1988. *Agrobacterium tumefaciens virE* operon encodes a single-stranded DNA-binding protein. Proc. Natl. Acad. Sci. USA **85**:2909–2913.
14. **de Bruijn, F. J., and J. R. Lupski.** 1984. The use of transposon Tn5 mutagenesis in the rapid generation of correlated physical and genetic maps of DNA segments cloned into multicopy plasmids—a review. Gene **27**:131–149.
15. **Engstrom, P., P. Zambryski, M. M. Van, and S. Stachel.** 1987. Characterization of *Agrobacterium tumefaciens* virulence proteins induced by the plant factor acetosyringone. J. Mol. Biol. **197**:635–645.
16. **Gutierrez, C., J. Barondess, C. Manoil, and J. Beckwith.** 1987. The use of transposon Tn*phoA* to detect genes for cell envelope proteins subject to a common regulatory stimulus. J. Mol. Biol. **195**:289–297.
17. **Hoffman, C. S., and A. Wright.** 1985. Fusions of secreted proteins to alkaline phosphatase: an approach for studying protein secretion. Proc. Natl. Acad. Sci. USA **82**:5107–5111.
18. **Kado, C. I.** 1993. *Agrobacterium*-mediated transfer and stable incorporation of foreign genes in plants, p. 243–254. *In* D. B. Clewell (ed.), Bacterial conjugation. Plenum Press, New York.
19. **Kellenberger, E., and M. A. Hayat.** 1991. Some basic concepts for the choice of methods, p. 1–30. *In* M. A. Hayat (ed.), Colloidal gold: principles, methods, and applications. Academic Press, Inc., San Diego, Calif.

20. **Kuldau, G. A.** 1991. Ph.D. thesis. University of California, Berkeley.
21. **Kuldau, G. A., V. G. De, J. Owen, G. McCaffrey, and P. Zambryski.** 1990. The *virB* operon of *Agrobacterium tumefaciens* pTiC58 encodes 11 open reading frames. Mol. Gen. Genet. **221:**256–266.
22. **Kyte, J., and R. F. Doolittle.** 1982. A simple method for displaying the hydropathic character of a protein. J. Mol. Biol. **157:**105–132.
23. **Lessl, M., D. Balzer, W. Pansegrau, and E. Lanka.** 1992. Sequence similarities between the RP4 *Tra2* and the Ti *VirB* region strongly support the conjugation model for T-DNA transfer. J. Biol. Chem. **267:**20471–20480.
24. **Maddock, J. R., and L. Shapiro.** 1993. Polar location of the chemoreceptor complex in the *Escherichia coli* cell. Science **259:** 1717–1723.
25. **Maniatis, T., E. F. Fritsch, and J. Sambrook.** 1982. Molecular cloning: a laboratory manual. Cold Spring Harbor Laboratory, Cold Spring Harbor, N.Y.
26. **Manoil, C., and J. Beckwith.** 1985. Tn*phoA*: a transposon probe for protein export signals. Proc. Natl. Acad. Sci. USA **82:**8129–8133.
27. **Matthysse, A. G., K. V. Holmes, and R. H. Gurlitz.** 1981. Elaboration of cellulose fibrils by *Agrobacterium tumefaciens* during attachment to carrot cells. J. Bacteriol. **145:**583–595.
28. **Melchers, L. S., T. T. Regensburg, R. B. Bourret, N. J. Sedee, R. A. Schilperoort, and P. J. J. Hooykaas.** 1989. Membrane topology and functional analysis of the sensory protein VirA of *Agrobacterium tumefaciens*. EMBO J. **8:**1919–1925.
29. **Okamoto, S., A. Toyoda-Yamamoto, K. Ito, I. Takebe, and Y. Machida.** 1991. Localization and orientation of the VirD4 protein of *Agrobacterium tumefaciens* in the cell membrane. Mol. Gen. Genet. **228:**24–32.
30. **Pansegrau, W., and E. Lanka.** 1991. Common sequence motifs in DNA relaxases and nick regions from a variety of DNA transfer systems. Nucleic Acids Res. **19:**3455.
31. **Pansegrau, W., G. Ziegelin, and E. Lanka.** 1990. Covalent association of the *traI* gene product of plasmid RP4 with the 5′-terminal nucleotide at the relaxation nick site. J. Biol. Chem. **265:**10637–10644.
32. **Russel, M., and B. Kaźmierczak.** 1993. Analysis of the structure and subcellular location of filamentous phage pIV. J. Bacteriol. **175:**3998–4007.
33. **Sambrook, J., E. F. Fritsch, and T. Maniatis.** 1989. Molecular cloning: a laboratory manual, 2nd ed. Cold Spring Harbor Laboratory Press, Cold Spring Harbor, N.Y.
34. **Shirasu, K., and C. I. Kado.** 1993. Membrane location of the Ti plasmid VirB proteins involved in the biosynthesis of a pilin-like conjugative structure on *Agrobacterium tumefaciens*. FEMS Microbiol. Lett. **111:**287–294.
35. **Shirasu, K., and C. I. Kado.** 1993. The *virB* operon of *Agrobacterium tumefaciens* virulence regulon has sequence similarities to B, C and D open reading frames downstream of the pertussis toxin-operon and to the DNA transfer-operons of broad-host-range conjugative plasmids. Nucleic Acids Res. **21:**353–354.
36. **Shirasu, K., Z. Koukolíková-Nicola, B. Hohn, and C. I. Kado.** 1993. An inner membrane associated virulence protein essential for T-DNA transfer from *Agrobacterium tumefaciens* to plants exhibits ATPase activity and similarities to conjugative transfer genes. Mol. Microbiol. **8:**641–650.
37. **Shirasu, K., P. Morel, and C. I. Kado.** 1990. Characterization of the *virB* operon of an *Agrobacterium tumefaciens* Ti-plasmid: nucleotide sequence and protein analysis. Mol. Microbiol. **4:**1153–1163.
38. **Stachel, S. E., G. An, C. Flores, and E. W. Nester.** 1985. A Tn3 *lacZ* transposon for the random generation of beta-galactosidase gene fusions: application to the analysis of gene expression in *Agrobacterium*. EMBO J. **4:**891–898.
39. **Stachel, S. E., and E. W. Nester.** 1986. The genetic and transcriptional organization of the *vir* region of the A6 Ti plasmid of *Agrobacterium tumefaciens*. EMBO J. **5:**1445–1454.
40. **Stachel, S. E., B. Timmerman, and P. C. Zambryski.** 1986. Generation of single-stranded T-DNA molecules during the initial stages of T-DNA transfer from *Agrobacterium tumefaciens* to plant cells. Nature (London) **322:**706–711.
41. **Stachel, S. E., and P. C. Zambryski.** 1986. *Agrobacterium tumefaciens* and the susceptible plant cell: a novel adaptation of extracellular recognition and DNA conjugation. Cell **47:**155–157.
42. **Tabor, S., and C. C. Richardson.** 1985. A bacteriophage T7 RNA polymerase/promoter system for controlled exclusive expression of specific genes. Proc. Natl. Acad. Sci. USA **82:**1074–1078.
43. **Thompson, D. V., L. S. Melchers, K. B. Idler, R. A. Schilperoort, and P. J. J. Hooykaas.** 1988. Analysis of the complete nucleotide sequence of the *Agrobacterium tumefaciens virB* operon. Nucleic Acids Res. **16:**4621–4636.

43a. **Thorstenson, Y. R., and R. Yson.** Unpublished data.

44. **Thorstenson, Y. R., and P. C. Zambryski.** 1993. Subcellular localization of seven VirB proteins of *Agrobacterium tumefaciens*: implications for the formation of a T-DNA transport structure. J. Bacteriol. **175:**5233–5241.
45. **Vestweber, D., and G. Schatz.** 1989. DNA-protein conjugates can enter mitochondria via the protein import pathway. Nature (London) **338:**170–172.
46. **Ward, J. E., D. E. Akiyoshi, D. Regier, A. Datta, M. P. Gordon, and E. W. Nester.** 1988. Characterization of the *virB* operon from an *Agrobacterium tumefaciens* Ti plasmid. J. Biol. Chem. **263:**5804–5814.
47. **Ward, J. E., D. E. Akiyoshi, D. Regier, A. Datta, M. P. Gordon, and E. W. Nester.** 1990. Correction: characterization of the *virB* operon from *Agrobacterium tumefaciens* Ti plasmid. J. Biol. Chem. **265:** 4768.
48. **Ward, J. E., Jr., E. M. Dale, P. J. Christie, E. W. Nester, and A. N. Binns.** 1990. Complementation analysis of *Agrobacterium tumefaciens* Ti plasmid *virB* genes by use of a *vir* promoter expression vector: *virB9*, *virB10*, and *virB11* are essential virulence genes. J. Bacteriol. **172:**5187–5199.
49. **Ward, J. E., Jr., E. M. Dale, E. W. Nester, and A. N. Binns.** 1990. Identification of a VirB10 protein aggregate in the inner membrane of *Agrobacterium tumefaciens*. J. Bacteriol. **172:**5200–5210.
50. **Waters, V. L., K. H. Hirata, W. Pansegrau, E. Lanka, and D. G. Guiney.** 1991. Correction: sequence identity in the nick regions of IncP plasmid transfer origins and T-DNA borders of *Agrobacterium* Ti plasmids. Proc. Natl. Acad. Sci. USA **88:**6388.
51. **Waters, V. L., K. H. Hirata, W. Pansegrau, E. Lanka, and D. G. Guiney.** 1991. Sequence identity in the nick regions of IncP plasmid transfer origins and T-DNA borders of *Agrobacterium* Ti plasmids. Proc. Natl. Acad. Sci. USA **88:**1456–1460.
52. **Weiss, A. A., F. D. Johnson, and D. L. Burns.** 1993. Molecular characterization of an operon required for pertussis toxin secretion. Proc. Natl. Acad. Sci. USA **90:**2970–2974.
53. **Winans, S. C.** 1992. Two-way chemical signaling in *Agrobacterium*-plant interactions. Microbiol. Rev. **56:**12–31.
54. **Winans, S. C., R. A. Kerstetter, J. E. Ward, and E. W. Nester.** 1989. A protein required for transcriptional regulation of *Agrobacterium* virulence genes spans the cytoplasmic membrane. J. Bacteriol. **171:**1616–1622.
55. **Zambryski, P. C.** 1992. Chronicles from the *Agrobacterium*-plant cell DNA transfer story. Annu. Rev. Plant Physiol. Plant Mol. Biol. **43:**465–490.
56. **Zambryski, P. C., H. Joos, C. Genetello, J. Leemans, M. Van Montagu, and J. Schell.** 1983. Ti plasmid vector for the introduction of DNA into plant cells without alteration of their normal regeneration capacity. EMBO J. **2:**2143–2150.
57. **Ziegelin, G., W. Pansegrau, B. Strack, D. Balzer, M. Kroger, V. Kruft, and E. Lanka.** 1991. Nucleotide sequence and organization of genes flanking the transfer origin of promiscuous plasmid RP4. DNA Sequence **1:**303–327.
58. **Zorick, T. S., and C. Schooley.** 1992. Ultrarapid freezing on a diamond surface. Microsc. Res. Tech. **20:**103–104.